Available online at www.eccomasproceedia.org
Eccomas Proceedia COMPDYN (2017) 2253-2268

ECCOMAS
Proceedia

COMPDYN 2017
6th ECCOMAS Thematic Conference on
Computational Methods in Structural Dynamics and Earthquake Engineering
M. Papadrakakis, M. Fragiadakis (eds.)
Rhodes Island, Greece, 15–17 June, 2017

DYNAMIC BEHAVIOUR OF THE SAN FELICE SUL PANARO FORTRESS: EXPERIMENTAL TESTS AND MODEL UPDATING

Marianna Forghieri, Elisa Bassoli and Loris Vincenzi

DIEF - University of Modena and Reggio Emilia
via Pietro Vivarelli, 10 41125 Modena
e-mail: marianna.forghieri@unimore.it, elisa.bassoli@unimore.it, loris.vincenzi@unimore.it

Keywords: Historical masonry structures, Ambient vibration testing, Dynamic identification, Model updating, Surrogate-assisted evolutionary algorithm.

Abstract. *This paper describes the experimental tests and numerical analyses performed to characterize the dynamic behaviour of the principal tower of the San Felice sul Panaro Fortress (Modena, Italy). After the Emilia earthquake that occurred in 2012, the Fortress reported serious damage, such as severe cracks on the walls and collapses of several towers and the roof. As a part of a research that aims at evaluating the vulnerability of the Fortress and designing retrofitting interventions, full-scale ambient vibration tests were performed to evaluate the dynamic properties of the principal tower. Afterwards, a Finite Element (FE) model is calibrated to obtain a good match between the numerical and experimental modal properties. The optimization process is carried out through an improved surrogate-assisted evolutionary strategy. Due to the serious damage of the Fortress, the effective stiffness of the cracked masonry and the efficiency of connection at the interface between the principal tower and the rest of the Fortress are considered the main uncertain quantities to be calibrated. A multi-objective optimization is performed, considering the frequency and mode shape residuals. These are defined as the difference between experimental and numerical modal properties. The multi-objective optimization is reduced to a series of a single-objective optimization adopting the weighted sum method. The set of optimal solutions that form the Pareto front is obtained performing the optimization for different values of the weighting factors. Then, two criteria are used and compared in order to find the preferred solution among the Pareto front solutions. Finally, a comparison of the identified structural parameters obtained varying the weighting factors for natural frequencies and mode shapes in the optimization process is presented, highlighting the importance of a proper choice of the weighting factors.*

Peer-review under responsibility of the organizing committee of COMPDYN 2017.
doi: 10.7712/120117.5564.17156

1 INTRODUCTION

Earthquakes occurred in Italy in the last decades have highlighted the vulnerability of historical buildings, such as churches, castles, masonry towers, etc. [1]. The assessment of the seismic vulnerability of historical buildings is still complex because these structures have a peculiar behaviour due to their own story and characteristics. The adoption of an accurate and calibrated numerical model [2], of proper mechanical characteristics of materials and of a suitable method of analysis are the keys to obtain reliable results. With this aim, Finite Element (FE) model updating allows to identify some uncertain parameters, such as mechanical characteristics of materials, by minimizing or maximizing some objective functions defined as the difference between numerical and experimental data.

In many optimization problems, especially those involving the calibration of numerical models with respect to experimental data, usually several objectives have to be fulfilled. In real-life problems, these objectives are often in conflict with each other due to the effect of measurement errors (whether experimental data are used) and model uncertainties (that are inaccuracies of the numerical model in reproducing the real behaviour of the structure). For this reason, to perform the optimization with respect to a single objective can lead to unacceptable results for the other objectives and thus a multi-objective optimization needs to be introduced.

There are two general approaches to handle multi-objective optimization. In the first approach, objectives are combined and weighted into a single-objective function [3]. Parametrically changing the weighting factors, all optimal solutions constituting the Pareto front can be easily obtained. The second approach is to solve directly the multi-objective problem avoiding the definition of weighting factors. Although several authors have proposed specific algorithms to solve directly the multi-objective optimization [4], the first approach is widely used due to its simpleness. Moreover, weighting factors give a physical meaning of the significance of each objective. Both approaches lead to define the Pareto front. Among the solutions of the front, the preferred one has to be defined using an appropriate decision making strategy [5, 6].

This paper describes the experimental tests and numerical analyses performed to characterize the dynamic behaviour of the principal tower of the San Felice sul Panaro Fortress (Modena, Italy). After the Emilia earthquake that occurred in 2012, the Fortress reported serious damage, such as severe cracks on the walls and collapses of several towers and the roof. This study is part of a research that aims at evaluating the vulnerability of the Fortress and designing retrofitting interventions. Full-scale ambient vibration tests were performed to evaluate the dynamic properties of the principal tower. During the tests, accelerometers were placed at several locations on the structure to collect the vibration response to natural excitation sources. Starting from the recorded accelerations, the classic Enhanced Frequency Domain Decomposition (EFDD) method is used to identify the experimental natural frequencies, mode shapes and damping ratios. Afterwards, a FE model of the Fortress is calibrated to obtain a good match between the numerical and experimental modal properties. Due to the serious damage pattern of the Fortress, the effective stiffness of the cracked masonry and the efficiency of connection at the interface between the tower and the rest of the Fortress are the main uncertain quantities to be calibrated. The set of optimal solutions that form the Pareto front is obtained reducing the multi-objective optimization to a series of a single-objective optimization. Each single-objective optimization is solved several times adopting the weighted sum method and changing the values of the weighting factors. The optimization process is carried out through an improved surrogate-assisted evolutionary strategy. Then, two criteria to find the preferred solution among the Pareto front solutions are adopted and compared. Finally, a comparison of the structural parameters identi-

(a) (b)

Figure 1: (a) The San Felice sul Panaro Fortress and (b) the "Mastio".

fied varying the weighting factors for natural frequencies and mode shapes in the optimization process is presented, highlighting the importance of a proper choice of the weighting factors.

2 THE SAN FELICE SUL PANARO FORTRESS

The San Felice sul Panaro Fortress is an historical masonry structures located in the town of San Felice sul Panaro (Modena, Italy). The main structure of the Fortress dates back to the XIV century, but as usual in ancient buildings, the Fortress was subjected to several transformations over the centuries [7, 8]. The current configuration of the Fortress is characterized by a quadrilateral plan with an inner yard and five towers (Fig. 1(a)). The highest tower is located on the south-east corner and it is called Mastio (Fig. 1(b)) due to its dominant dimensions compared to the rest of the building.

The Fortress has been seriously damaged by the seismic sequence that affected the Emilia land in May 2012. Two main shocks occurred on May 20$^{\text{th}}$ and May 29$^{\text{th}}$ with magnitude of M_L = 5.9 and M_L = 5.8, respectively. Both epicentres were a few kilometers far from the Fortress. Due to the 2012 earthquake, the roofs of the four minor towers collapsed and many cracks of different relevance appeared on the walls of the Fortress [1]. Important shear cracks occurred in the Mastio and some vertical cracks appeared between the Mastio and the perimeter walls. In addition, relevant damage can be observed in the merlons as well as in the vaults inside the Mastio.

Soon after the seismic events, the municipality of San Felice sul Panaro performed some strengthening interventions in order to prevent further collapses. The diagonal cracks of the Mastio were filled with mortar and steel strands were inserted into the walls.

3 DYNAMIC IDENTIFICATION

Ambient vibration tests were performed in July 2016 to measure the response of the Mastio in operational conditions and to identify its modal properties. Because the Fortress reported serious damage after the 2012 earthquake, the modal identification refers to the dynamic behaviour of the Mastio in damaged conditions.

A total of 10 uniaxial piezoelectric accelerometers (7 PCB/393B12 and 3 PCD393/B31), were installed at four levels of the Mastio on the inner walls, as shown in Figure 2. At the upper level (L4) sensors were mounted in different positions with respect to the lower levels

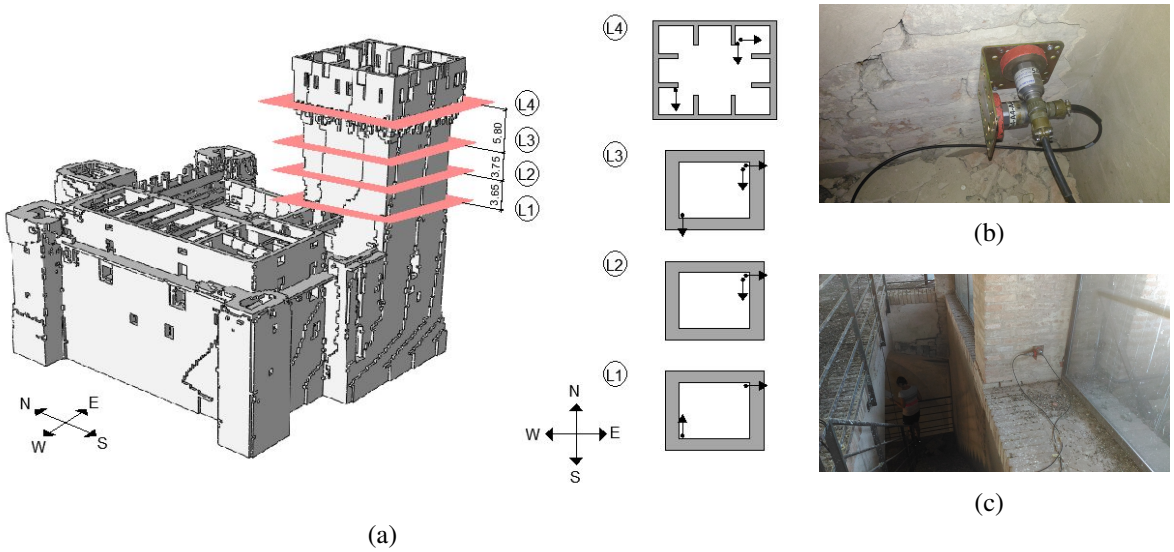

Figure 2: Ambient vibration tests: (a) instrumented cross-sections and sensor location; accelerometers at level (b) L3 and (c) L4 in the N-E corner.

because of the different position of the masonry walls (Fig. 2(a)). The accelerometers have a dynamic range of $\pm$ 0.5 g, a bandwidth ranging form 0.15 to 1000 Hz and a resolution of 8 µg (PCB/393B12) and 1 µg (PCB/393B31). They were connected to a National Instruments acquisition system for data storage and system management. The sampling frequency was set to 200 Hz.

The Enhanced Frequency Domain Decomposition method is used to identify the modal properties of the Mastio from the ambient vibration data [9, 10]. The Power Spectral Density (PSD) matrix of the acquired accelerations is calculated and decomposed with the Singular Value Decomposition (SVD) method. Each singular vector of the PSD matrix represents the *j*-th mode shape whereas each singular value is the amplification factor, i.e. the structural response amplification under dynamic loads. Each peak of the PSD graph identifies the natural frequency of each mode. Finally, the damping ratio is estimated through the logarithmic decrement.

An example of acceleration time series recorded at the upper level and its corresponding PSD function are presented in Figures 3(a) and 3(b), respectively. The measured acceleration ranges between $\pm$ 5 mg (corresponding to $\pm$ 0.05 m/s^2), stating the low level of ambient excitation that existed during the tests.

Four bending modes and a torsional one are clearly identified. The mode shapes of the identified modes and the corresponding modal properties (natural frequencies and damping ratios) are reported in Figure 4 and Table 1. The first two bending modes involve flexure in the E-W direction (Fig. 4(a)) and N-S direction (Fig. 4(b)), respectively, while the third mode is a torsional mode (Fig. 4(c)). The forth (Fig. 4(d)) and fifth mode (Fig. 4(e)) are second bending modes characterized by dominant flexure in N-S and E-W direction, respectively.

4 FINITE ELEMENT MODEL OF THE SAN FELICE SUL PANARO FORTRESS: MODEL UPDATING AND STRUCTURAL IDENTIFICATION

A detailed FE model of the San Felice sul Panaro Fortress (Fig. 5) has been developed by Castellazzi et al. [11] adopting an innovative numerical modelling strategy. The strategy

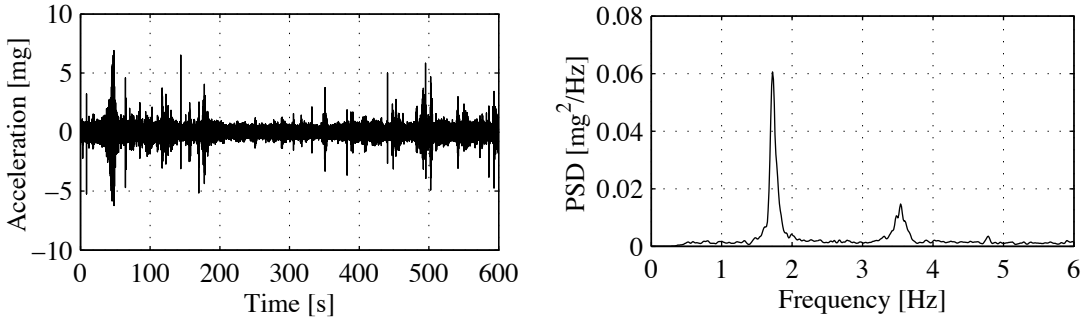

Figure 3: (a) Acceleration recorded at level L4 and (b) corresponding PSD function.

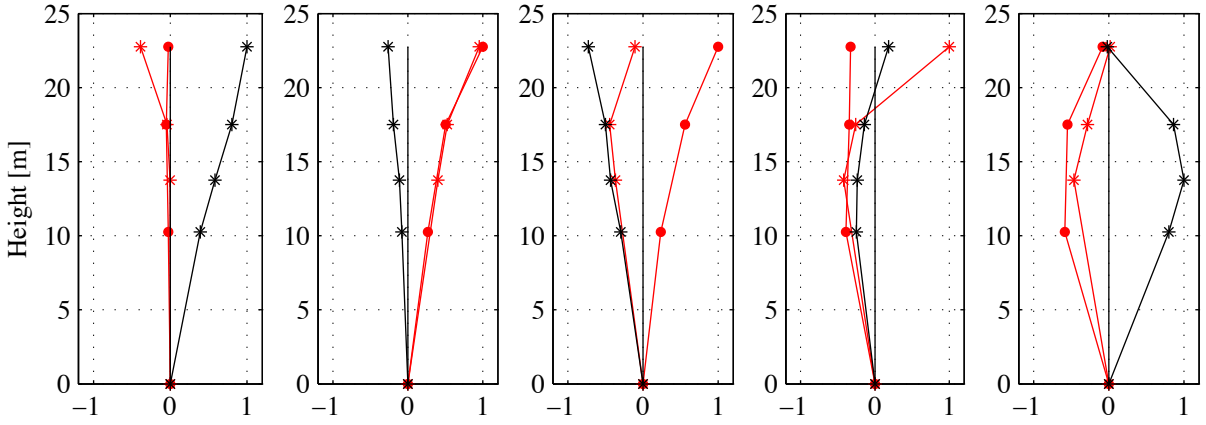

Figure 4: Mode shapes of the (a, b, d, e) bending and (c) torsional modes. Black asterisks: modal displacements of the measuring points in the N-E corner of the cross-section in E-W direction; Red asterisks: modal displacement of the N-E corner in N-S direction; Red dots: modal displacement of the W-S corner in N-S direction.

enables the semi-automatic transformation of a three-dimensional point cloud of a structure into a three-dimensional point FE mesh. The survey of all the external and internal surfaces of the Fortress was performed after the 2012 earthquake by using a terrestrial laser scanner [2]. Therefore, the FE model represents the post-earthquake condition of the monument. The details of the new semi-automatic procedure to transform three-dimensional point clouds of complex objects into three-dimensional FE models can be found in [11].

In the present section, the FE model of the Fortress is calibrated so that the modal properties of the Mastio agree as close as possible with the experimental ones. To this end, some uncertain structural parameters are identified from the minimization of an objective function that measures the difference between experimental data and numerical predictions. In particular, the elastic modulus of the masonry and the elastic moduli of the elements at the interface between the Mastio and the rest of the Fortress on the west and north side are selected as uncertain structural parameters. The interface elements on the west and north side are called “Connection A” and “Connection B”, respectively, and highlighted in Figures 5(a) and 5(b). The choice of the

Mode shape	Frequency [Hz]	Damping Ratio [%]
1st Bending E-W	1.72	2.31
1st Bending N-S	1.75	3.40
1st Torsional	3.55	2.24
2nd Bending N-S	4.83	0.99
2nd Bending E-W	5.08	0.94

Table 1: Modal properties of identified modes.

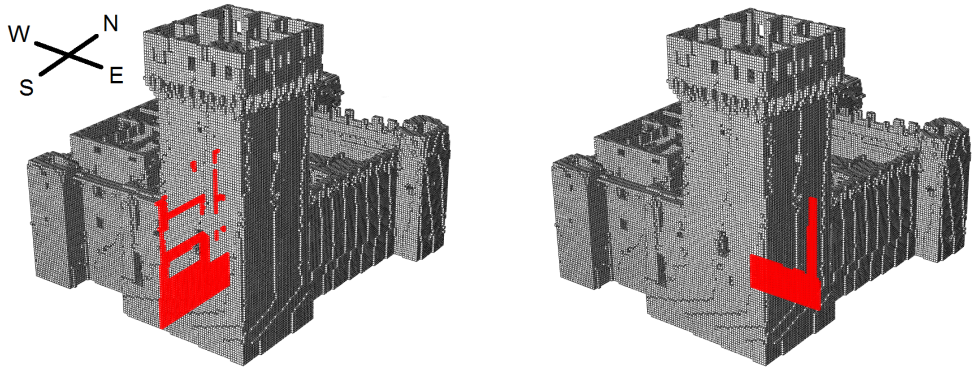

(a) Connection A (b) Connection B

Figure 5: Elements at the interface between the Mastio and the perimeter walls: (a) on the west side; (b) on the north side.

uncertain structural parameters is related to the age of the construction and the serious damage caused by the 2012 earthquake. The elastic modulus of the masonry can be considered as an equivalent elastic modulus of the cracked masonry of the Mastio. Moreover, the Fortress had a complex historical evolution and consequently the monolithic behaviour and the efficiency of connection between adjacent walls cannot be assured. Furthermore, important cracks can be observed in correspondence of the interfaces between the Mastio and the rest of the Fortress.

An improved surrogate-assisted evolutionary strategy, named DE-S algorithm [12] and described in section 4.2, is adopted to calibrate the FE model of the Fortress. The first three natural modes of the Mastio are accounted for in the calibration procedure, i.e. the first bending modes in the two orthogonal directions and the torsional one. The numerical modes involving the Mastio are shown in Figure 6. In section 4.3, the optimization problem is solved defining the objective function as the weighted sum of frequency and mode shape residuals. The Pareto front is then calculated by solving several optimization problems for different weighting factors. Two criteria to find the best solution among the points of the Pareto front are described and compared, namely the maximum bend angle [5] and the minimum distance [13] criterion. The impact of the weighting factor on the optimal solution is also highlighted. Results are presented and compared in section 4.4.

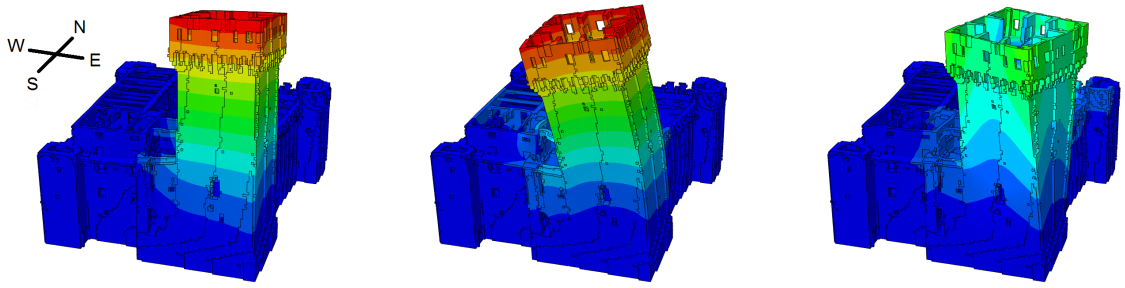

(a) 1st bending N-S (b) 1st bending E-W (c) 1st torsional

Figure 6: Numerical mode shapes.

4.1 Single- and multi-objective optimization

In many optimization problems, especially those involving the calibration of numerical models with respect to (real) experimental data, usually several objectives have to be fulfilled. Moreover, in real-life problems, these objectives are often in conflict with each other. This is due to (i) the uncertainties and errors that unavoidably affect the numerical model and (ii) the presence of uncertainties in the measurements. For this reason, to perform the optimization with respect to a single objective can lead to unacceptable results for the other objectives.

To address this issue, a multi-objective optimization problem, which involves more than one objective function to be optimized simultaneously, has to be introduced. Multi-objective optimization problems can be handled with two general approaches. The first relies on a reduction of the multi-objective optimization problem into a single-objective problem adopting, for instance, the weighted sum method [3]. This method defines the objective function to be minimized as the weighted sum of different objectives. Depending on the weighting factor assigned to each objective, the optimization procedure can lead to different results because of the uncertainties and errors affecting the numerical model and the measurements. Hence, a proper definition of the weighting factor is not trivial. The set of optimal solutions that form the Pareto front [14] can be obtained solving the optimization problem several times for different weighting factors. The Pareto front represents a set of feasible non-inferior solutions that are not dominated by any one. An objective on the Pareto front can not be improved without sacrificing at least one other objective. The second approaches is based on the resolution of a multi-objective optimization problem to directly obtain the entire Pareto front or a representative subset of it. For this purpose, specific multi-objective genetic algorithms can be adopted (see [4] for an extensive overview of these methods). In both approaches, once the Pareto front is defined, a decision is still required to find the solution that is the best compromise among the different objectives. The best solution among the points that constitute the Pareto front is selected on the basis of additional (sometime subjective) requirements.

In dynamic structural identification, the goal is to identify a set of uncertain structural parameters such that the numerical properties agree as close as possible with the experimental ones. In this work, the objectives are defined in terms of frequency e_F and mode shape e_M residuals:

$$e_F = \sum_{i=1}^{N} \left(\frac{f_{num,i} - f_{exp,i}}{f_{exp,i}} \right)^2 \tag{1}$$

$$e_M = \sum_{i=1}^{N} \left(\frac{1 - MAC(\phi_{num,i}, \phi_{exp,i})}{MAC(\phi_{num,i}, \phi_{exp,i})} \right)^2 \tag{2}$$

where N is the number of modes selected for the calibration, $f_{exp,i}$ and $\phi_{exp,i}$ are the experimental frequencies and mode shapes, respectively, $f_{num,i}$ and $\phi_{num,i}$ are the numerical frequencies and mode shapes and MAC is the well-known Modal Assurance Criterion [15].

4.2 The DE-S algorithm

Genetic and evolutionary algorithms are widely used for solving global optimization problems. Their architecture is designed for large-scale problems and allows to avoid local minima. The main drawback is that a large number of function evaluations is often required to reach the convergence. Surrogate-assisted evolutionary strategies [16] use efficient computational models, such as Response Surfaces (RS), high polynomial functions or Kriging models [17], to approximate the objective function. They aim at evaluating those individuals that potentially have a good prediction of the objective function value. The introduction of a second-order surrogate in the Differential Evolution (DE) algorithm is proposed in [18].

In the DE-S algorithm, proposed by [12], a proper infill sampling strategy is introduced to further reduce the number of objective function evaluations. The candidate points are chosen trying to find a compromise between local and global search, i.e. enhancing both the accuracy in the region of the optimum predicted by the surrogate (local exploitation) and the global exploration. The DE-S algorithm is briefly summarized in the following.

First, the objective function is evaluated for the initial population. At each subsequent iteration, subsets of points are built and a quadratic response surface is calibrated for each subset *i*. If the *i*-th response surface is convex, the *i*-th Mutant vector is defined as the minimum of the surrogate function. On the contrary, if the *i*-th response surface is concave, the Mutant vector is obtained form a linear combination of the population vectors and the Crossover operation is performed to increase the diversity of vectors and avoid local optima. Each Mutant vector represents a candidate point for a new evaluation. A score w is assigned to each candidate (Scoring operation). Only a limited number of points are selected for new evaluations depending on their scores.

The score is defined as the weighted sum of two criteria. The first depends on the objective function value predicted by the surrogate while the second depends on the distances of the candidate from the points where the objective function has already been evaluated. For this purpose, a database containing both the position of the previously evaluated points and the associated objective function values is created. The new favourite candidates can be placed in between or far from the previously evaluated points.

The reader referred to [12] for all details about the DE-S algorithm.

4.3 Evaluation of the preferred solution from the Pareto front

The calibration of the FE model aims at minimizing the differences between the numerical and experimental results, in terms of both natural frequencies and mode shapes. According to the weighting sum method, the objective function H is defined as follows:

$$H = \alpha e_F + (1 - \alpha) e_M \tag{3}$$

where α is the weighting factor that measures the relative importance between the two objectives e_F and e_M (Eqs.1 and 2).

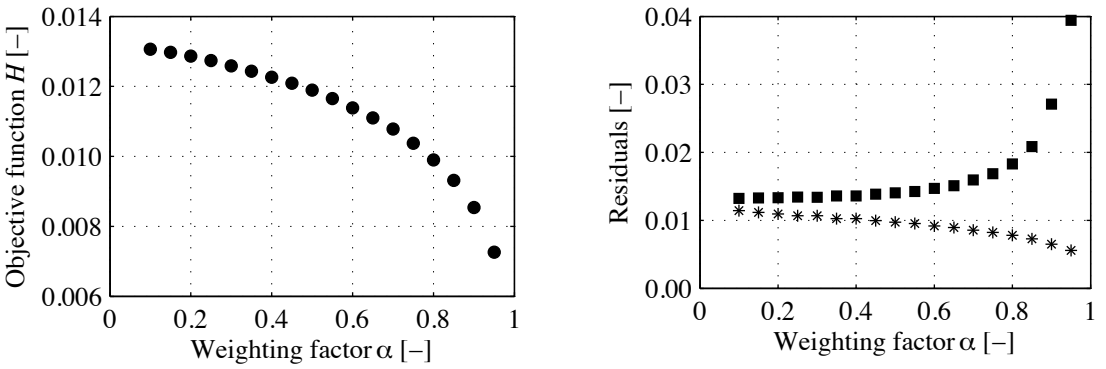

(a) (b)

Figure 7: Results of the weighted sum method: trend of (a) the objective function H and (b) the natural frequency (asterisks) and mode shape (squares) residuals with the weighting factor α.

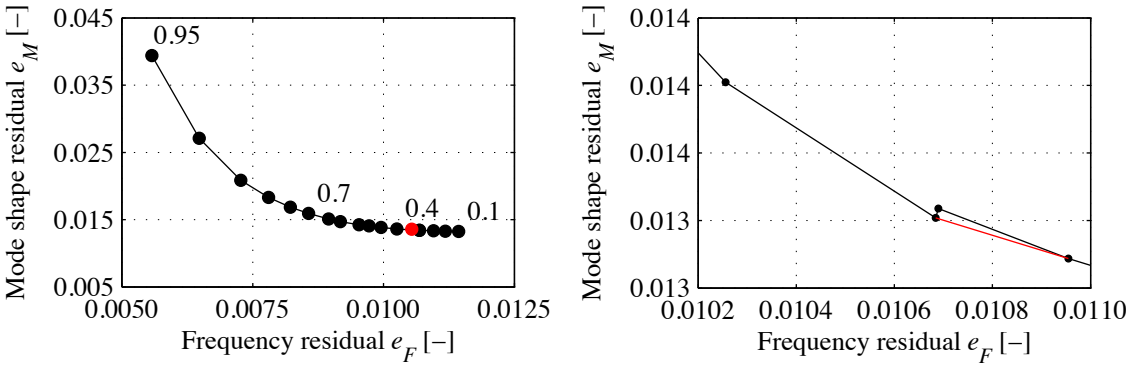

(a) (b)

Figure 8: (a) Pareto front for different values of α (black dots) and optimal solution for the objective function Δ (red dot); (b) detail of an "irregularity" of the Pareto front.

The optimization analysis is repeated for different weighting factors α to obtain the Pareto front. Values of α ranging between 0.1 and 0.95 with step size 0.05 are adopted. For each value of α, the optimal elastic moduli of the masonry E_M and of the interface elements E_A and E_B that minimize the objective function H are evaluated. Values of H, e_F and e_M obtained for different α are reported in Figure 7. When α increases H and e_F decrease while e_M increases. It is observed that, as mentioned before, the two objectives e_F and e_M do not guide the problem to a unique solution. On the contrary, each objective leads to a different combination of optimal structural parameters.

Figure 8 shows the Pareto front, obtained representing the calculated residuals in the objective function space. Each marker represents a solution of the weighted sum method, i.e. each marker is related to a specific value of the weighting factor α.

Among the solutions obtained for different values of α, the best one needs to be identified. The solution corresponding to the minimum value of H might not be the best one. As shown in Figure 7(a), the minimum value of H is obtained when $\alpha = 0.95$, i.e. when almost only the contribution of the frequency residual is accounted for. The contribution of the mode shape

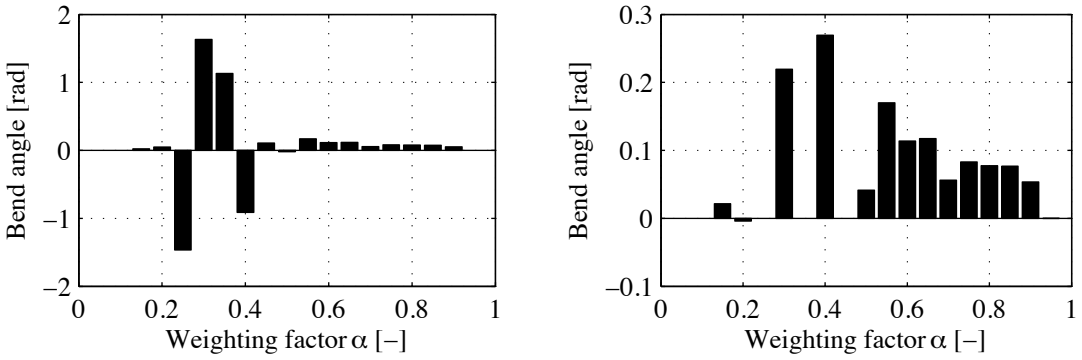

(a) (b)

Figure 9: Values of the bend angle for each point of the Pareto front (a) before and (b) after removing the "irregularities".

residual, which in this case provides the greatest source of error, is multiplied by a factor of 0.05 and so it is almost disregarded. Therefore, a criterion to select the solution that is the best compromise between the two objectives is needed. For this purpose, two criteria are presented and compared in this paper.

First, the formulation proposed by [5] is adopted. The best solution (named "SOL-A" in the following) is identified as the point of the Pareto front with the maximum bend angle. For this solution, a large sacrifice is required to make a small gain to move to any other solution. The bend angle β of a solution k on the Pareto front depends on the slopes of the two lines connecting k with its adjacent left L and right R neighbours. The bend angle of the k-th solution is computed as:

$$\beta(k) = \beta_L - \beta_R \tag{4}$$

where:

$$\beta_L = \arctan\left[\frac{e_M(k-1) - e_M(k)}{e_F(k) - e_F(k-1)}\right] \tag{5}$$

and

$$\beta_R = \arctan\left[\frac{e_M(k) - e_M(k+1)}{e_F(k+1) - e_F(k)}\right]. \tag{6}$$

$k-1$ and $k+1$ are the previous (left) and following (right) solution of the considered point k, respectively.

Values of the bend angle obtained from Eq.4 for each point of the Pareto front are reported in Figure 9(a).

The convergence of the optimization procedure is reached when prescribed convergence criteria are satisfied. Small inaccuracies in the solution for a given value of α can cause sharp changes of slopes in the Pareto front, as shown in Figure 9(b). In correspondence of these points, high values of bend angle are obtained, which are related to the inaccuracy in the definition of the front and not to effective preferred solutions. If these "irregular" points are removed from the Pareto front (i.e. the red line is considered instead of the black one in Figure 8(b)), the maximum bend angle is obtained for $\alpha = 0.4$ (Fig. 9(b)) instead of $\alpha = 0.3$ (Fig. 9(a)).

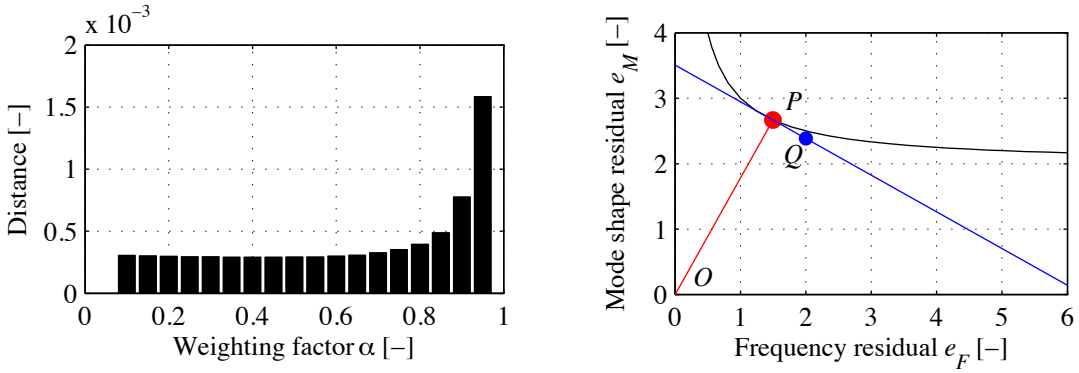

(a) (b)

Figure 10: (a) Distance of each point of the Pareto front from the origin; (b) tangent line (blue) to the Pareto front (black) at the point P and line perpendicular to the tangent line (red).

However, the result obtained by this criterion strongly depends on the accuracy in the definition of the front as well as on the subjective evaluation of the "irregular" points of the front.

Another criterion to evaluate the optimal solution on the Pareto front is investigated in this paper. The best solution is defined as the point of the Pareto front with minimum distance from the origin (named "SOL-D" in the following) [13]. The origin of the objective function space represents the ideal solution because it is characterized by frequency and mode shape residuals equal to zero. Thus, the minimum distance from the origin ensures the best compromise between frequency and mode shape errors. Figure 10(a) shows the distance of each point of the Pareto front from the origin. The minimum distance, and so the best solution, is obtained for $\alpha = 0.4$.

This solution is consistent with the one obtained from the maximum bend angle criterion once the "irregularities" of the front are removed. Unlike the maximum bend angle criterion, the minimum distance is less affected by the presence of "irregular" points on the front. However, in this case, the minimum distance criterion provides a set of solutions characterized by almost the same distance from the origin, while the optimal solution can be more clearly identified with the maximum bend angle criterion.

The same result obtained by the minimum distance criterion can also be achieved directly, avoiding the computation of the whole Pareto front. This implies to perform a single optimization analysis instead of several analyses for different values of α. To this aim, a new single-objective function Δ that represents the distance of a given point in the objective function space from the origin is defined:

$$\Delta = \sqrt{e_F^2 + e_M^2} \tag{7}$$

The optimal solution obtained by the minimization of Eq.7 is characterized by a frequency residual $e_F(P) = 0.0105$ and a mode shape residual $e_M(P) = 0.0136$. The optimal solution, represented in Figure 8(a) with a red dot, lies on the Pareto front previously evaluated close to the solutions with $\alpha = 0.4 \div 0.5$.

The objective function Δ does not include explicitly the weighting factor α. The value of α corresponding to the estimated solution can be evaluated as follows. Let's consider the generic Pareto front defined in the objective function space and reported in Figure 10(b). The point of the Pareto front with the minimum distance from the origin is indicated as P. According to

the Taylor's theorem, the Pareto front around the point P can be approximated by a first order Taylor polynomial. The tangent line to the Pareto front at the point P (blue line in Fig. 10(b)) is perpendicular to the segment OP and is formulated as:

$$e_M = e_M(P) - \frac{e_F(P)}{e_M(P)}(e_F - e_F(P)) \tag{8}$$

Hence, the coordinates of a point Q on the tangent line (Eq. 8) close to P are given by:

$$e_F(Q) = e_F(P) + \varepsilon, \quad e_M(Q) = e_M(P) - \frac{e_F(P)}{e_M(P)}\ \varepsilon \tag{9}$$

where it is assumed that $e_F(Q) - e_F(P) = \varepsilon$, with ε a very small number. According to Eq.3, the objective functions H evaluated in P and Q are written:

$$\begin{cases} H(P) = \alpha_P\ e_F(P) + (1-\alpha_P)\ e_M(P) \\ H(Q) = \alpha_Q\ e_F(Q) + (1-\alpha_Q)\ e_M(Q) \end{cases} \tag{10}$$

Being ε a very small number, it is assumed that the points P and Q have almost the same values of weighting factor α and objective function H:

$$\begin{cases} H(P) \approx H(Q) \\ \alpha(P) \approx \alpha(Q) \end{cases} \tag{11}$$

Finally, substituting Eqs.9 and 11 into Eq.10, an estimate α^* of the weighting factor α related to the optimal solution is obtained:

$$\alpha^* = \frac{\gamma}{1+\gamma} \tag{12}$$

where $\gamma = e_F(P)/e_M(P)$.

From Eq.12, a weighting factor α^* equal to 0.437 is obtained. This is in line with the weighting factor estimated from the minimum distance criterion, namely $\alpha = 0.4$. The slight discrepancy between the results can be explained as follows. First, the solution obtained from the minimum distance criterion depends on the accuracy of the Pareto front (i.e. the step size of α). Second, some assumptions are made in the procedure to evaluate α^*, which are: (i) the Pareto front is approximated by a first order Taylor polynomial and (ii) the values of H and α for the points P and Q are assumed to be the same.

In summary, the presented strategy allows to accurately evaluate the optimal solution, and thus the uncertain structural parameters, with no need to compute the whole Pareto front. Moreover, the relative importance between the frequency and mode shape residuals for the estimated solution can be easily evaluated.

4.4 Structural parameter identification

This section presents and compares the structural parameters and the modal properties obtained from the optimization analyses reported in section 4.3. Optimal weighting factors α, frequency e_F and mode shape e_M residuals and the corresponding structural parameters obtained by the maximum bend angle (SOL-A) and the minimum distance (SOL-D) criterion are listed in Table 2. Being the optimal weighting factors obtained by the two criteria in very good agreement, the residuals and the structural parameters are very similar as well.

	α [-]	e_F [10^{-2}]	e_M [10^{-2}]	E_M [MPa]	E_A [MPa]	E_B [MPa]
SOL-A	0.4	1.026	1.361	937	35	10
SOL-D	0.437	1.054	1.359	912	43	11
SOL-F	1	0.106	48.31	862	27	2083

Table 2: Results obtained by the maximum bend angle criterion (SOL-A), by the minimum distance criterion (SOL-D) and considering only the frequency residual (SOL-F).

		SOL-A			SOL-D			SOL-F		
Mode Shape	Exp. Freq. [Hz]	Num. Freq. [Hz]	Rel. Error [%]	MAC [%]	Num. Freq. [Hz]	Rel. Error [%]	MAC [%]	Num. Freq. [Hz]	Rel. Error [%]	MAC [%]
1st B. E-W	1.72	1.76	−2.32	94.4	1.76	−2.00	95.3	1.71	0.53	64.0
1st B. N-S	1.75	1.61	8.58	91.9	1.59	9.29	91.9	1.71	2.57	71.2
1st T.	3.55	3.72	−4.85	95.4	3.68	−3.88	95.4	3.61	−1.93	94.1

Table 3: Experimental and numerical modes obtained by the maximum bend angle criterion (SOL-A), by the minimum distance criterion (SOL-D) and considering only the frequency residual (SOL-F). 1st B. E-W: first bending mode in E-W direction; 1st B. N-S: first bending mode in N-S direction; 1st T.: first torsional mode.

Results of the FE model calibration show that the elastic modulus of the masonry E_M is about 920 MPa, while the elastic moduli E_A and E_B of the interface models are about 40 MPa and 10 MPa, respectively. As expected, the cracked masonry has a low elastic modulus due to its poor quality and the damage suffered by the 2012 earthquake. The elastic moduli of the interface elements suggest low, but not absent, level of connection between the Mastio and the rest of the Fortress.

The calibrated FE models show very similar modal characteristics ("SOL-A" and "SOL-D" in Table 3). The values of frequency relative errors, lower than 9.3%, and MAC, greater than 91%, state the good agreement between numerical and experimental modes.

The importance of a proper choice of the weighting factor is highlighted in Figure 11 that shows the trends of the elastic moduli obtained by the weighted sum method for different values of α. See for instance that when $\alpha = 0.95$ (i.e. when the weight of frequency residual is dominant with respect to the mode shape residual), the elastic moduli of the interface elements are nearly one order of magnitude higher than their mean values (that are less than 50 MPa).

Finally, results obtained considering only the frequency residual in the optimization process (i.e. $\alpha = 1$) are presented. These are referred to as "SOL-F" in Tables 2 and 3. In this case, the optimal solution shows even more pronounced differences with the solutions obtained for $\alpha < 1$, in terms of both structural parameters and modal properties. In particular, while the frequency errors decrease up to values lower than 2.6%, the MAC drops to unacceptably low level, with values of 63% and 71% for the first two bending modes.

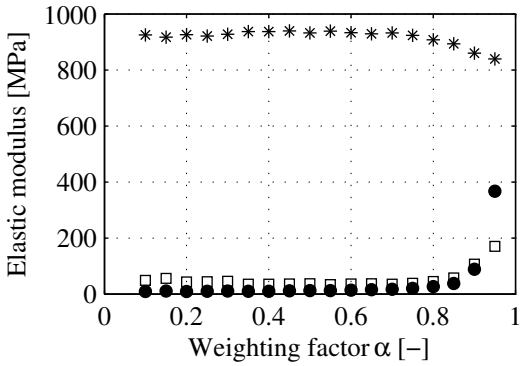

Figure 11: Variation of elastic moduli as a function of the weighting factor α: elastic modulus of Connection A (squares), elastic modulus of Connection B (dots), and elastic modulus of masonry (asterisks).

5 CONCLUSIONS

The paper addresses the modal and parameter identification of the San Felice sul Panaro Fortress. Results of ambient vibration tests and the FE model optimization are presented. The modal characteristics of the principal tower (Mastio) are identified from ambient vibration data by means of the Enhanced Frequency Domain Decomposition method. Afterwards, an optimization process is performed to identify the elastic modulus of the cracked masonry of the Mastio and the elastic moduli of the elements at the interface between the Mastio and the perimeter walls. On this account, an objective function which combines the relative errors between experimental and numerical modal properties is formulated. The Pareto front is determined solving the optimization problem several times for different values of the factor weighting the frequency and mode shape residuals.

Two criteria to identify the preferred FE solution among those constituting the Pareto front are presented. The first criterion identifies the best solution as the point on the Pareto front with the maximum bend angle. In the second one, the preferred solution is that with the minimum distance from the origin of the objective function space. For the minimum distance criterion, a strategy that allows to evaluate the optimal solution with no need to compute the whole Pareto front is also presented.

Results show that the two criteria give almost the same value of the weighting factor. Indeed, the values of frequency residual, mode shape residual and mechanical properties of the materials are almost coincident. In both cases, modal properties obtained by the calibration process are in good agreement with the experimental ones.

The result obtained by the maximum bend angle criterion strongly depends on the accuracy in the definition of the Pareto front as well as on the subjective evaluation of the "irregular" points of the front. As a matter of fact, small inaccuracies in the solution for a given value of the weighting factor can cause sharp changes of slopes in the Pareto front and, thus, large variation in the identified best solution. Unlike the maximum bend angle criterion, the minimum distance criterion is less sensitive to the presence of irregularities on the front shape. However, in the analysed case-study, several solutions are characterized by almost the same distance from the origin and the preferred solution does not clearly prevails on the others.

The importance of a proper choice of the weighting factor is finally highlighted. When the weight of frequency residual is dominant with respect to mode shape residual, the elastic moduli of the interface elements are nearly one order of magnitude higher than those obtained with

a moderate value of the weighting factor. Moreover, if only frequencies are used in the optimization process, the calibrated FE model provides very inaccurate mode shapes. In summary, optimization results suggest that, in this case, the best compromise is obtained when the weight of mode shape residual is slightly higher than the weight of natural frequency residual.

REFERENCES

[1] S. Cattari, S. Degli Abbati, D. Ferretti, S. Lagomarsino, D. Ottonelli, and A. Tralli, "Damage assessment of fortresses after the 2012 Emilia earthquake (Italy)," *Bulletin of Earthquake Engineering*, vol. 12, no. 5, pp. 2333–2365, 2014.

[2] G. Castellazzi, A. M. D'Altri, S. de Miranda, and F. Ubertini, "An innovative numerical modeling strategy for the structural analysis of historical monumental buildings," *Engineering Structures*, vol. 132, pp. 229–248, 2017.

[3] I. Kim and O. de Weck, "Adaptive weighted-sum method for bi-objective optimization: Pareto front generation," *Structural and Multidisciplinary Optimization*, vol. 29, no. 2, pp. 149–158, 2005.

[4] A. Konak, D. W. Coit, and A. E. Smith, "Multi-objective optimization using genetic algorithms: A tutorial," *Reliability Engineering and System Safety*, vol. 91, no. 9, pp. 992 – 1007, 2006.

[5] S. S. Jin, S. Cho, H. J. Jung, J. J. Lee, and C. B. Yun, "A new multi-objective approach to finite element model updating," *Journal of Sound and Vibration*, vol. 333, no. 11, pp. 2323 – 2338, 2014.

[6] N. Wang, W. Jie Zhao, N. Wu, and D. Wu, "Multi-objective optimization: A method for selecting the optimal solution from pareto non-inferior solutions," *Expert Systems with Applications*, vol. 74, pp. 96 – 104, 2017.

[7] A. Orlando, "Rocca Estense a San Felice sul Panaro. Modellazione e analisi del suo comportamento sismico," Master's thesis, Genoa: Univestity of Genoa, 2014. (in italian).

[8] L. Ferrari and G. Goldoni, "Dietro il Segno. Dentro e fuori il restauro della Rocca di San Felice sul Panaro," Master's thesis, Parma: University of Parma, 2014. (in italian).

[9] R. Brincker, L. Zhang, and P. Andersen, "Modal identification of output-only systems using frequency domain decomposition," *Smart Materials and Structures*, vol. 10, no. 3, p. 441, 2001.

[10] R. Brinker, C. Ventura, and P. Andersen, "Damping estimation by frequency domain decomposition," in *Proceedings of the 19th International Modal Analysis Conference*, (San Antonio, Texas, USA), 2001.

[11] G. Castellazzi, A. M. D'Altri, G. Bitelli, I. Selvaggi, and A. Lambertini, "From laser scanning to finite element analysis of complex buildings by using a semi-automatic procedure," *Sensors*, vol. 15, no. 8, pp. 18360–18380, 2015.

[12] L. Vincenzi and P. Gambarelli, "A proper infill sampling strategy for improving the speed performance of a Surrogate-Assisted Evolutionary Algorithm," *Computers and Structures*, vol. 178, pp. 58–70, 2017.

[13] G. Sun, G. Li, Z. Gong, X. Cui, X. Yang, and Q. Li, "Multiobjective robust optimization method for drawbead design in sheet metal forming," *Materials and Design*, vol. 31, no. 4, pp. 1917 – 1929, 2010.

[14] V. Pareto, *Manuale di Economia Politica*. Societa Editrice Libraria, Milano, Italy, 1906. (in italian). Translated into English by A.S. Schwier: *Manual of Political Economy*, Macmillan, New York, 1971.

[15] R. Allemang and D. Brown, "A correlation coefficient for modal vector analysis," in *Proceedings of the 1st International Modal Analysis Conference*, (Orlando, Florida, USA), pp. 110–116, 1982.

[16] Y. Jin, "Surrogate-assisted evolutionary computation: Recent advances and future challenges," *Swarm and Evolutionary Computation*, vol. 1, no. 2, pp. 61 – 70, 2011.

[17] J. Müller, C. A. Shoemaker, and R. Pich, "SO-MI: A surrogate model algorithm for computationally expensive nonlinear mixed-integer black-box global optimization problems," *Computers & Operations Research*, vol. 40, no. 5, pp. 1383 – 1400, 2013.

[18] L. Vincenzi and M. Savoia, "Coupling response surface and differential evolution for parameter identification problems," *Computer-Aided Civil and Infrastructure Engineering*, vol. 30, no. 5, pp. 376–393, 2015.